



ARCHIVES
of
FOUNDRY ENGINEERING

DOI: 10.1515/afe-2017-0061

Published quarterly as the organ of the Foundry Commission of the Polish Academy of Sciences

ISSN (2299-2944)
Volume 17
Issue 2/2017

111 – 118

Numerical Simulation of Directional Solidification Process of Single Crystal Ni-Based Superalloy Casting

D. Szeliga *, **K. Kubiak**, **J. Sieniawski**Faculty of Mechanical Engineering and Aeronautics, Rzeszow University of Technology
Ul. W. Pola 2, 35-959 Rzeszów

*Corresponding author: E-mail address: dszeliga@prz.edu.pl

Received 05.07.2016; accepted in revised form 29.09.2016

Abstract

The analysis of influence of mould withdrawal rate on the solidification process of CMSX-4 single crystal castings produced by Bridgman method was presented in this paper. The predicted values of temperature gradient, solidification and cooling rate, were determined at the longitudinal section of casting blade withdrawn at rate from 1 to 6mm/min using ProCAST software. It was found that the increase of withdrawal rate of ceramic mould results in the decrease of temperature gradient and the growth of cooling rate, along blade height. Based on results of solidification parameter G/R (temperature gradient/solidification rate), maximum withdrawal rate of ceramic mould (3.5 mm/min), which ensures lower susceptibility to formation process of new grain defects in single crystal, was established. It was proved that these defects can be formed in the bottom part of casting at withdrawal rate of 4 mm/min. The increase of withdrawal rate to 5 and 6 mm/min results in additional growth of susceptibility of defects formation along the whole height of airfoil.

Keywords: Numerical simulation, Single crystal, CMSX-4 Ni-based superalloys, ProCAST, Casting defects

1. Introduction

Nickel superalloys are widely used in manufacture of aircraft engine and industrial gas turbine hot-section components which are working under heavy loads and are especially exposed to factors responsible for inducing hot corrosion and thermal fatigue [1, 2]. The turbine blades and vanes are produced mostly by investment casting method [3, 4].

The manufacture of castings by directional solidification method is based on the withdrawal of ceramic mould poured with molten metal, at a certain rate from the heating zone to the cooling area of furnace [5, 6]. In this way, positive value of the temperature gradient and a movement of the solidification front along the height of the casting can be achieved. The positive

temperature gradient in the casting can be obtained by the application of directional heat flow in the casting through intense cooling of the mould part located below the heating area of furnace. The methods that are used on industrial scale for manufacturing single crystal nickel based superalloy castings have been developed: Bridgman, LMC (Liquid Metal Cooling) and GCC (Gas Cooling Casting), depending on the cooling process.

Two different production techniques of single crystal castings of nickel based superalloys with predetermined crystallographic orientation are usually applied, of which grain selector or seed technique are frequently used [1]. The use of a grain selector can provide the growth of one grain in the whole volume of casting in particular crystallographic direction [001]. The shape of selector has changed with the development of technology of single crystal

castings. Currently, the most commonly used is a spiral grain selector. The application of a starter and selector allows the solidification of casting grains of crystallographic orientation [001] close to symmetry axis. The crystallographic orientation other than [001] is often required in the single crystal castings [7]. It was observed that the manufacturing of castings of orientation near to [111] further improved its creep resistance. The nickel based superalloy single crystal castings of predetermined crystallographic orientation are manufactured using casting seed. The method is used to control the orientation of the single crystal casting produced on industrial and on laboratory scale [8].

Temperature gradient, solidification and cooling rates determine the shape of solidification front and microstructure of morphology of single crystal castings [9]. The increase of cooling rate leads to the reduction of secondary dendrite arm spacing, fragmentation of eutectic island ($\gamma+\gamma'$) and γ' precipitate particles as well as the decrease of duration and cost of heat treatment process. The temperature gradient and solidification rate influence the formation of defects (freckle, low and high angle grain boundary, stray grain), especially in nickel superalloys single crystal castings [10]. Thus, there is a tendency to raise the temperature gradient and cooling rate of castings, as well as the increase of the withdrawal rate of the mould in order to produce the single crystal casting with lower susceptibility to defect formation and decreased cost production [11].

The areas of defect formation in single crystal castings are often predicted using numerical simulation of solidification process [12-18]. The effect of mould withdrawal rate on the formation of stray grains in platform blades is usually analyzed by applying macro-scale 3D Cellular Automaton Finite Element (CAFE) model. The heterogeneous nucleation coefficients such as the values of undercooling ΔT of the formation of stray grains in the bulk metal and at the surface of mould as well as growth rate of dendrite tip depending on ΔT for the nickel based superalloy are required in this method. Their values are particularly difficult to determine experimentally.

The local solidification parameters (temperature gradient G and solidification rate R), are often determined in the areas of casting defects in order to understand better the phenomenon of their creation [19, 20]. It was found, that the stray grains and freckles form in the SX1 superalloy of single crystal rod at the critical values parameters of $G/R < 2700 \text{ K s/cm}^2$ [19]. The value of parameter G/R can be determined using numerical simulation. Hence, the potential areas of defect formation in the single crystal casting blades can be predicted through the critical value of parameter G/R determined experimentally earlier.

Therefore, in this paper the maximum withdrawal rate of mould, which ensures lower susceptibility to defect formation and better control of solidification of CMSX-4 nickel based single crystal casting produced with the Bridgman method is determined applying the G/R criterion.

2. Methodology

The numerical simulations of the temperature distribution and solidification parameters in the castings depending on withdrawal rate of mould were conducted with the use of the ProCAST software. The three-dimensional model assembly and the

ambience of ceramic shell mould were designed. The assembly consists of 5 starters, 5 selectors, 5 blades, a gating system, pouring cup and chill plate. The casting blade contains of a continuer, airfoil, platform and root (Fig.1).

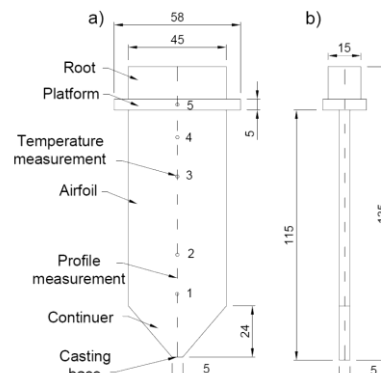


Fig. 1. The geometric model of casting blade and temperature measurements points (1÷5)

The construction of the vacuum furnace, used for manufacturing the single crystal castings with the Bridgman method, was a basis for creating the three-dimensional ambience model of ceramic shell mould. The ambience describes the internal space of the heating and cooling area. The geometric model of the heating chamber contains the inner surface of two heaters with diameter of 300 mm and the upper plate of the thermal insulation. The model of the thermal insulation layer was 30 mm thick and of internal diameter 250 mm. It was placed on chill rings, in the lower part of the furnace heating area. The cooling area of the furnace consisted of the inner surface of chill rings with the diameter of 250 mm and the cooling chamber with the diameter of 594 mm (Fig. 2c). The model of radiation baffle was additionally created in the three-dimensional ambience of the ceramic mould (Fig. 2b). This model with the internal diameter of 220 mm and thickness of 2.5 mm was placed on the thermal insulation plate.

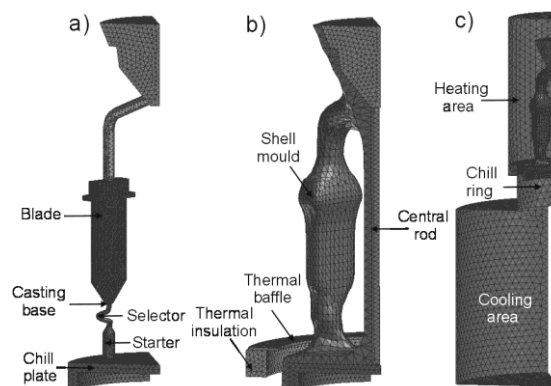


Fig. 2. The finite elements mesh: a) model assembly, b) shell mould and both thermal baffle and insulation, c) surface of the melting (heating) and the cooling area of furnace and mould

The geometric model assembly and the three-dimensional ambience of ceramic shell mould were divided into 5 parts. The

three-dimensional finite elements mesh was generated at 1/5 of the model assembly (Fig. 2a), thermal insulation and the radiation baffle (Fig. 2b). The layer of ceramic shell mould with thickness of about 9 mm was created at the model assembly (Fig. 2b). Additionally, the finite elements mesh of surface was generated at heating and cooling area of ceramic shell mould ambience (Fig. 2c).

The materials and suitable values of thermophysical parameters (specific heat, density, thermal conductivity) were assumed for the geometric models of ceramic shell mould, insulation and radiation baffle [3, 5, 11]. The CMSX-4 nickel based superalloy was used for the models of casting rods and gating system. The thermophysical parameters of superalloys and values of liquidus (1380 °C) as well as solidus (1320 °C) temperatures were assumed on the basis of literature [21].

The suitable boundary conditions at 2 and 3D geometric model were applied during the simulation [22]. The surface temperature of heating area was equal to 1520 °C. The temperature of the chill ring and the cooling area was assumed to be 20 °C. The emissivity value of the surfaces of both heater and insulation (graphite) was equal to $\epsilon=0.85$ and for ceramic shell mould of $\epsilon=0.8$. The value of emissivity on the surface of chill rings and the internal surface of cooling area was $\epsilon=0.7$ and $\epsilon=0.5$, respectively [23]. The surface heat transfer coefficient of $h=5000$ W/m²K and temperature of 20 °C at internal surface of the chill plate (cooling water) was assumed. The value of interface heat transfer coefficient was fixed to be $h=20$ W/m²K on the contact surface of the ceramic shell mould and the casting, on the contact surface of casting and the chill plate. The constant value of $h=200$ W/m²K was assumed for the remaining interface [5, 11].

The simulation of preheating of the ceramic mould and the thermal insulation was executed, until the constant temperature (1520 °C) in their cross-section was reached. After the appropriate duration of heating, the mould was poured with liquid alloy (1510 °C) and afterwards withdrawn from the heating to cooling area of the furnace at rates of 1÷6 mm/min.

The boundary conditions and thermophysical parameters assumed in the simulations were experimentally verified comparing both, the predicted and the experimental cooling curves at the withdrawal mould rate of 3 mm/min. To do so, the single crystal casting blades were produced using Bridgman method at the withdrawal rate of 3 mm/min. The temperature measurements were carried out in 5 points using type B thermocouples (PtRh6 and PtRh30) with the diameter of 0.2 mm, which were placed along the symmetry axis of the blade at the distance of 29, 47, 83, 101, 116 mm from the casting base (Fig.1). The production technique of moulds and castings as well as the method of temperature measurements were discussed more precisely by Szeliga et al [3-5, 24].

The solidification parameters, such as: temperature gradient G, solidification rate R and cooling rate v was determined using the ProCAST software on the basis of predicted value of temperature distribution. In order to characterize the kinetics of casting solidification process, the average cooling rate for the time range between reaching liquidus and solidus temperatures (alloy solidification process) was determined based on equation:

$$v = \frac{\Delta T}{\Delta t} = \frac{T_L - T_S}{t_L - t_S} \quad (1)$$

where: T_L and T_S – liquidus and solidus temperature, t_L and t_S – time of reaching the liquidus and solidus temperature.

The temperature gradient was determined at the liquidus isotherm (solidification front). It was assumed, that the rate of movement of liquidus isotherms, determined the solidification rate R. The values of solidification parameters of G/R in the analyzed castings were determined applying the RGL criteria with the use of ProCAST software. The RGL criterion (referred also as mapping factor) was defined by the following equation:

$$M = aR^b G^c v^d \quad (2)$$

where: G – temperature gradient, K/cm; R – solidification rate, cm/s; v – cooling rate K/s. For the assumed coefficients values: $a=1$, $b=-1$, $c=1$ and $d=0$, the equation (2) defines solidification parameters:

$$M = G/R \quad (3)$$

3. Results

3.1. Temperature distributions

The numerical simulation was used for establishing the temperature distribution in the casting, ceramic shell mould and both heating and cooling areas (Fig. 3 a, b, c). Based on those results, cooling rate, temperature gradient, solidification rate, solidification parameter G/R and maximum withdrawal rate of casting, manufactured with Bridgman method were determined.

The temperature distributions were also established experimentally at the withdrawal casting rate of 3 mm/min. Those measurements were the basis for the verification of temperature distribution along the height of blade. A good agreement of experimental and predicted cooling curves was found, especially in the upper part of the blade (3-5 points). It confirmed that the values of thermophysical parameters and boundary conditions were appropriately assumed in the simulations.

It was observed on the basis of cooling curves, that few seconds after pouring, the liquid metal heats up to the maximum temperature as the result of thermal interaction of mould and metal. Then cooling of the alloy is performed by the withdrawal of the ceramic shell mould from the heating to cooling area of the furnace. Between the liquidus and solidus temperature the shape of curve changes, especially for the root and platforms (points 7 and 6). The solidification process starts, when the liquid metal reaches the liquidus. There is an intensive solidification of γ phase crystals accompanied by additional release of transition heat. The intensity of solid phase formation is the highest during the initial stage of transition. Afterwards, it decreases gradually until the solidification temperature of eutectic in nickel superalloy is reached. The solidification process ends at the solidus point (1320 °C).

3.2. Cooling rate

The average cooling rate in the mushy zone was determined along the height of casting blade withdrawn at rate from of 1 to 6

mm/min (Fig. 4, 5). It was found that the cooling rate attained the largest value in the connection area of casting base and selector

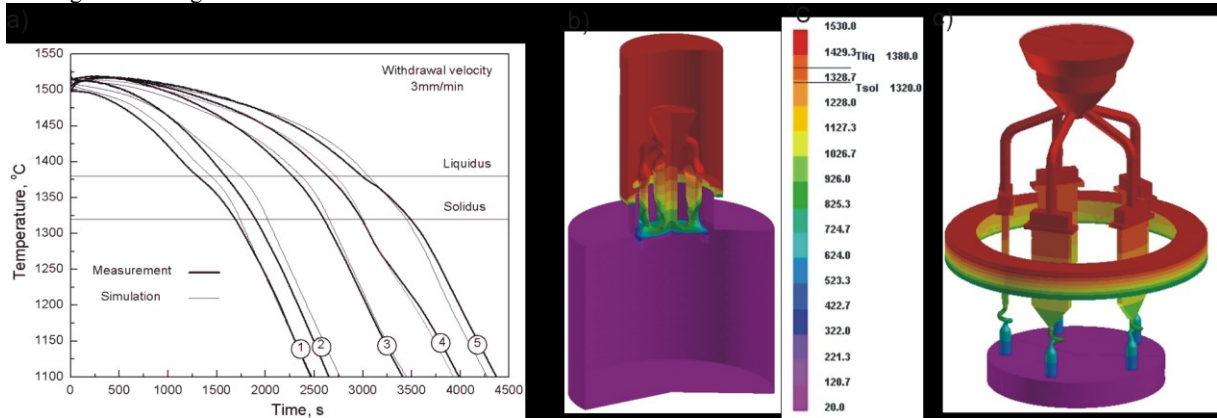


Fig. 3. The predicted and measured temperature distribution along the height of casting blade (a, c) and shell mould with heating and cooling areas after 1650s from start of pouring (b) and withdrawal rate of 3 mm/min. 1÷5 – temperature test points depending on distance to casting base (1÷4 –airfoil, 5 – platform)

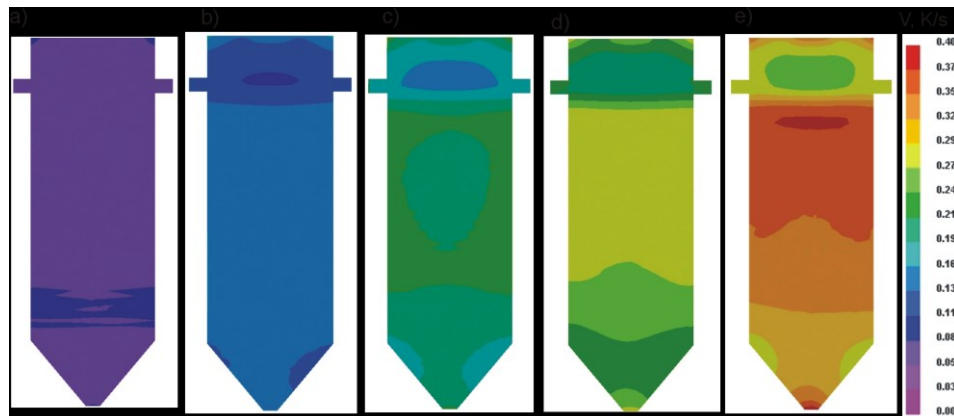


Fig. 4. The cooling rate along the height of casting blade for withdrawal rates: a) 1, b) 2, c) 3, d) 4 and e) 6 mm/min

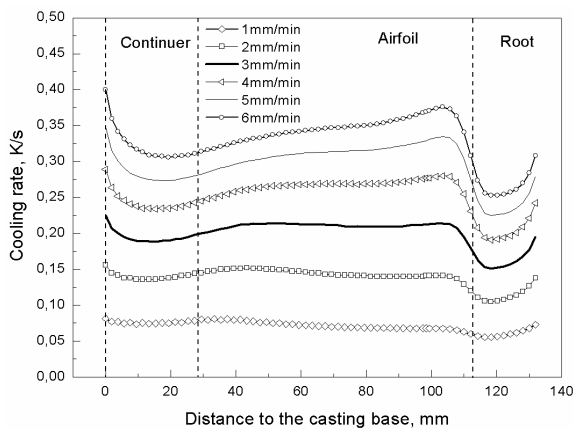


Fig. 5. The cooling rate along the height of casting blade for withdrawal rates from 1 to 6 mm/min

The cooling rate significantly decreases with increasing distance from the casting base and in about half of the continuer its value in the connection area of casting base and selector.

The cooling rate significantly decreases with increasing distance from the casting base and in about half of the continuer its value again increases. Above the distance of approx. 40 mm from the casting base, the value of cooling rate becomes constant for the withdrawal rate of 1÷3 mm/min and slightly increases for other rates. It was found, that the thickness of casting affects cooling rate. Its value significantly decreases below the platform and in the area of cross-section change (airfoil/platform transition). The increase of withdrawal rate of casting causes increasing differences of cooling rate between the airfoil and root. The most homogeneous distribution of cooling rate along the height of casting is achieved for the withdrawal rate of 1 mm/min. However, the cooling rate depends mostly on withdrawal rate of casting. Increasing the withdrawal rate brings about significant growth of cooling rate along the height of blade. The average

value of cooling rate is equal to 0.7, 0.23 and 0.31 K/s for withdrawal rate of 1, 3 and 6 mm/min, respectively.

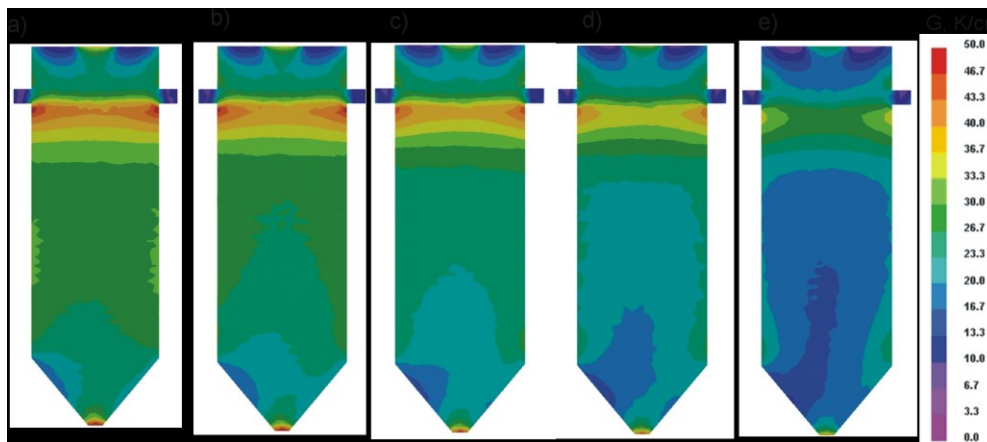


Fig. 6. The temperature gradient at liquidus isotherm along the height of casting blade for withdrawal rates: a) 1, b) 2, c) 3, d) 4 and e) 6 mm/min

3.3. Temperature gradient

The distribution of temperature gradient at the liquidus isotherm was determined along the height of blades, which were withdrawn at rates from of 1 to 6 mm/min (Fig. 6). The values were obtained along the symmetry axis of blade (Fig. 7). It has been found that the temperature gradient achieves the largest value in the connection area of selector and casting base, which was approx. 45 and 55 K/cm for the withdrawal rate of 1 and 6 mm/min, respectively. Its values significantly reduce in the continuer of blade to minimum values for distance approx. 13 mm from the casting base. Above this distance, the value of the temperature gradient gradually increases. In the upper part of blade at height of approx. 80 mm the temperature gradient considerably grows and its maximum value is attained in the area of cross-section change (airfoil/platform transition). Its value increases in the volume of airfoil below the platform in spite of constant thickness of casting. Thus, it was concluded that the temperature gradient in the analyzed area depends significantly on size of platform and root of blade. The increase of the root and platform blade thicknesses causes a significant drop of temperature gradient to the value similar to that of the airfoil. It has been found, that temperature gradient almost does not change along the airfoil height, regardless of the withdrawal rate. However, each change of cross-section of casting causes a large change of temperature gradient and conditions of solidification process. The temperature gradient – like the cooling rate – also depends on withdrawal rate of casting. The critical withdrawal rate, which would allow obtaining the maximum value of temperature gradient in the casting was not found. Its value increased in the whole volume of casting by about a similar value (approx. 4 K/cm at the distance of 60 mm from the casting base) with lowering withdrawal rate.

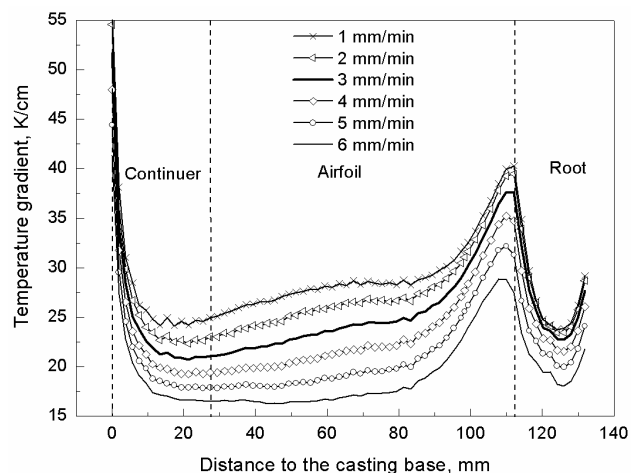


Fig. 7. The temperature gradient at liquidus isotherm along the height of casting blade for withdrawal rates from 1 to 6 mm/min

3.4. Solidification rate

The shifting rate of the liquidus isotherms was defined along the symmetry axis of blade, which was withdrawn at rate from of 1 to 6 mm/min (Fig. 8). It was assumed in the paper that the liquidus isotherm assumes the position of solidification front. Therefore the shifting rate determines the solidification rate of casting. It was found that the solidification rate takes different values along the height of blade compared with the withdrawal rate of casting. The solidification rate increases in the connection area of the selector and casting base and then it attains the maximum value. For distances greater than 10 mm from the casting base, its value gradually decreases to the smallest value in the area of cross-section change (airfoil/platform transition). The gradual change of solidification rate in the airfoil – despite of the

same thickness – is a result of the application of selector and change of the heat flow during the withdrawal of mould.

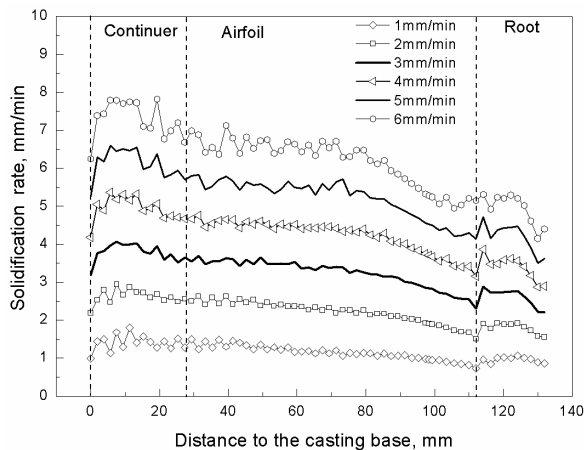


Fig. 8. The solidification rate along the height of casting blade for withdrawal rates from 1 to 6 mm/min

4. Discussion

The solidification parameters such as cooling rate v , temperature gradient G and solidification rate R influence the formation both of casting defects and dendritic microstructure in nickel based superalloys of single crystal casting blades. Therefore, the critical value of the parameter solidification G/R is often determined during the formation of casting defects [19, 20].

Pollock and Murphy [19] reported that the stray grains and freckle were formed in the SX1 superalloy of single crystal rod for the value of $G/R < 2700 \text{ K s/cm}^2$. However, the lateral growth of dendrite appears for values $G/R < 3500 \text{ K s/cm}^2$ for the CMSX-486 superalloys [20]. The increase of solidification parameter G/R ensures a lower susceptibility to defect formation.

The predicted value of G/R distribution was obtained on the surface of longitudinal section of casting blade and

along the symmetry axis at withdrawal rate from 1 to 6 mm/min (Fig. 10, 11). It has been found that the largest value of the solidification parameter G/R was obtained at a sudden change of cross-section of blade, although the lowest value of G/R was established at the bottom part of casting, in the continuer. The increase of withdrawal rate of casting brought about the reduction of the G/R value.

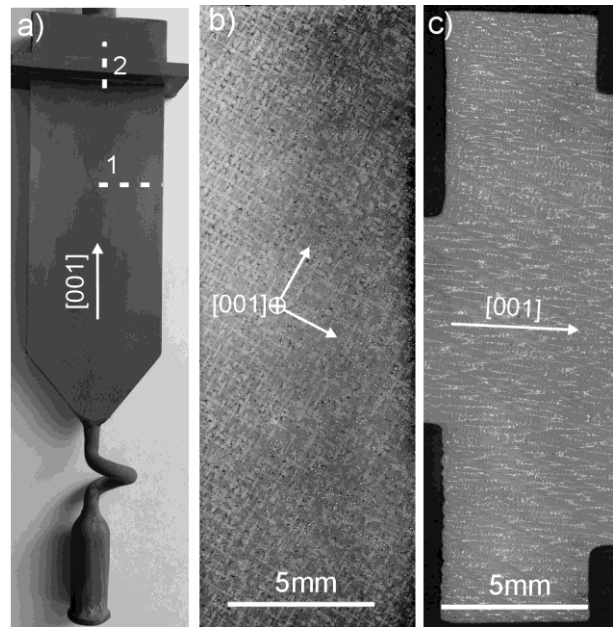


Fig. 9. The macrostructure on the surface (a) and microstructure on cross section of airfoil (b) as well as longitudinal section of platform and root (c) for blade withdrawn with rate of 3mm/min. [001] - the growth direction of dendrite trunks, 1 - cross section, 2 - longitudinal section

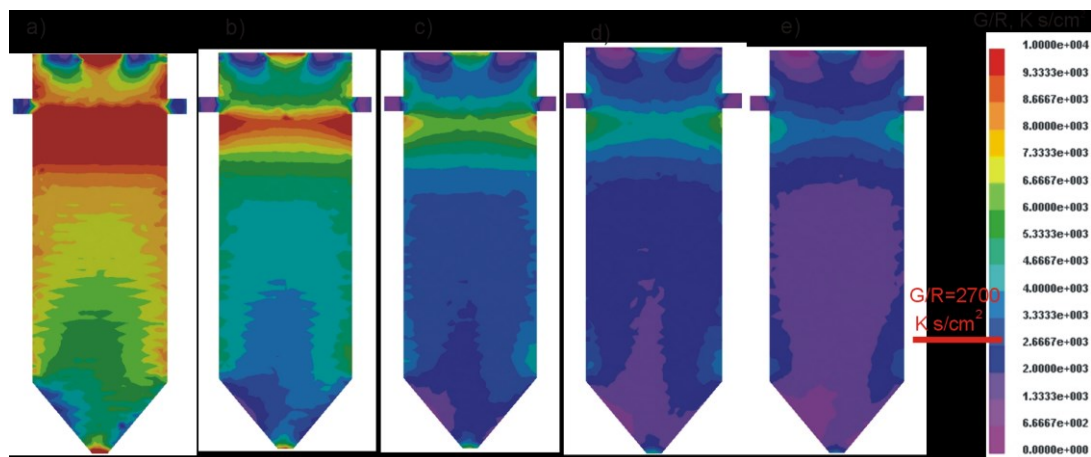


Fig. 10. The solidification parameters G/R along the height of casting blade for withdrawal rates: a) 2, b) 3, c) 4, d) 5 and e) 6 mm/min

The predicted formation areas of casting defects were determined through the numerical simulation of parameter G/R and experimentally determined critical value of G/R [19]. It was found that defects can be formed in the bottom part of blade at withdrawal rate of 4 mm/min (Fig. 11). The increase of withdrawal rate to 5 and 6 mm/min additionally elevated the susceptibility of defect formation along the whole height of airfoil. The lowest susceptibility of defect formation occurs for castings which are withdrawn at low rate (1 and 2 mm/min). However, the time and production cost of such castings is the highest. Therefore, the most suitable casting withdrawal rate is 3 mm/min. The typical defects, in the single crystal blade withdrawn at the rate of 3 mm/min, were not observed in the micro- and macrostructure examinations (Fig.9). The dendrites in the platform, root and airfoil had a correct shape and their growth in [001] direction was close to the symmetry axis of blade (Fig.9b, c). Therefore, the resulting parameter of G/R and macro- and microstructure show that it is possible to increase the withdrawal rate to 3.5 mm/min or even 4 mm/min, which allows an additional reduction of the production time and cost of castings. The predicted critical withdrawal rate was compared with the results reported in the literature [25-28]. The analysis of literature results indicates that suggested withdrawal rates of castings are contained in the range 2.5 to 6 mm/min depending on the shape of casting. Elliott et al [25] produced large blades at the withdrawal rate of 2.5 mm/min. Miller and Pollock [26] used the rate of 2.5 and 3.4 mm/min for the vanes (CMSX-486) of 51 and 19 mm thicknesses, respectively. However, the casting rods of diameter $10 \div 12$ mm were usually withdrawn at 3.4 mm/min [27, 28].

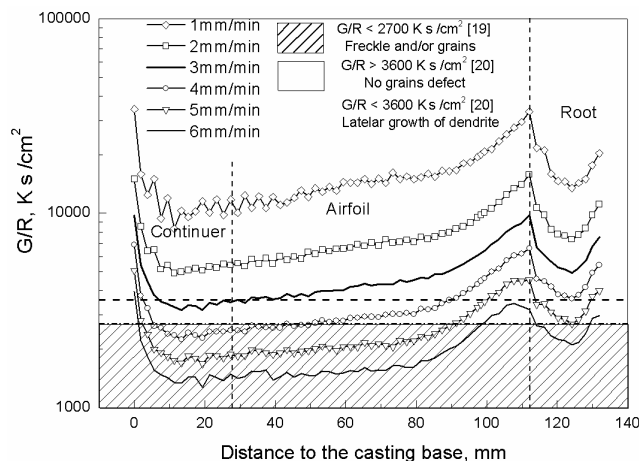


Fig. 11. The solidification parameters G/R along the height of casting blade for withdrawal rates from 1 to 6 mm/min

5. Conclusions

Based on the analysis of research results, the following conclusions were drawn:

1. The increase of withdrawal rate of ceramic mould causes decrease of temperature gradient and increase of cooling rate along the height of blade.

2. The solidification rate is usually characterized by another value along the blade height in comparison with the withdrawal rate of casting.

3. The maximum withdrawal rate of mould was determined on the basis of G/R criterion to be 3.5 mm/min, which ensures lower susceptibility to the formation of new grain defect.

4. The defects can form in the bottom part of casting at withdrawal rate of 4 mm/min. The increase of withdrawal rate to 5 and 6 mm/min additionally increases the susceptibility to defects formation along the whole height of airfoil.

Acknowledgements

The paper was written on the basis of research project financed by the National Science Centre (DEC-2013/09/N/ST8/02042).

References

- [1] Kubiak, K., Szeliga, D., Sieniawski J. & Onyszko, A. (2015). The Unidirectional Crystallization of Metals and Alloys (Turbine Blades). P Rudolph (Eds.), *Handbook of Crystal Growth: Bulk Crystal Growth (Second Edition)*. 413-457. Elsevier. DOI: 10.1016/B978-0-444-63303-3.00011-0.
- [2] Fraś, E., Guzik, E., Kapturkiewicz, W. & López, H.F. (1996). Processing and microstructure of investment casting turbine blade NITAC in-situ composites. Thermal and Mechanical Processing. *Journal of Materials Engineering and Performance*. 5(1), 103-110. DOI: 10.1007/BF02647277.
- [3] Szeliga, D., Kubiak, K., Ziaja, W. & Cygan, R. (2014). Influence of silicon carbide chills on solidification process and shrinkage porosity of castings made of nickel based superalloys. *International Journal of Cast Metal Research*. 27(3), 146-160. DOI: 10.1179/1743133613Y.0000000092
- [4] Szeliga, D., Kubiak, K., Cygan, R., Ziaja W. (2012). Application of Silicon Carbide Chills in Controlling the Solidification Process of Casts Made of IN-713C Nickel Superalloy. *Archives of Foundry Engineering*. 12(spec.2), 105-111.
- [5] Szeliga, D., Kubiak, K. & Sieniawski, J. (2016). Control of liquidus isotherm shape during solidification of Ni-based superalloy of single crystal platforms. *Journal of Materials Processing Technology*. 232(8), 18-26. DOI: 10.1016/j.jmatprotec.2016.03.003
- [6] Fraś, E., Guzik E. & Lopez, H.F. (1988). Structure and mechanical properties of unidirectionally solidified Fe-Cr-C and Fe-Cr-X-C alloys. *Metallurgical Transactions A*. 19(5), 1235-1241. DOI: 10.1007/BF02662584.
- [7] D'Souza, N., Jennings, P.A., Yang, X.L., Lee, P.D., McLean, M. & Dong, H.B. (2005). Seeding of single-crystal superalloys – role of constitutional undercooling and primary dendrite orientation on stray-grain nucleation and growth. *Metallurgical and Materials Transactions B*. 36(5), 657-666. DOI: 10.1007/s11663-005-0056-6
- [8] Toloraiya, V.N., Orekhov, N.G., Kablov, E.N. (2002). Advanced method for single crystal casting of turbine blades for gas turbine engines and plants. *Metal Science and Heat*

- Treatment*. 44(7), 279–283. DOI: 10.1023/A:1021299619346.
- [9] Glowina, J. & Janas, A. (1987). Microsegregation in dendritic single crystals of nickel-rich alloys. *Materials Science and Technology*. 3(2), 149-154. DOI: 10.1179/mst.1987.3.2.149.
- [10] Chmiela, B., Szeliga, D., Sozańska, M., Jarczyk, J. & Cwajna, J. (2013). Analysis of stray grain formation in single crystal CMSX-4 superalloy. *Practical Metallography*. 50(8), 548–560. DOI: 10.3139/147.110225.
- [11] Szeliga, D., Kubiak, K. & Jarczyk, G. (2013). The influence of the radiation baffle on predicted temperature gradient in single crystal CMSX-4 castings. *International Journal of Metalcasting*. 7(3), 17-23. DOI: 10.1007/BF03355555.
- [12] Yu, J., Xu Q., Liu, B., Li, J., Yuan, H. & Jin, H. (2008). Experimental Study and Numerical Simulation of Directionally Solidified Turbine Blade Casting. *J. Mater. Sci. Technol.* 24(3), 369-373.
- [13] Xu, Q., Liu, B., Pan, D. & Yu, J. (2012). Progress on modeling and simulation of directional solidification of superalloy turbine blade casting. *China Foundry*. 9(1), 69-77.
- [14] Xu, Q., Zhang, H. & Qi, X. (2014). Multiscale Modeling and Simulation of Directional Solidification Process of Turbine Blade Casting with MCA Method. *Metall. and Mater. Trans. B*. 45(2) 555-561. DOI:10.1007/s11663-013-9909-6.
- [15] Yu, J., Xu, Q. Y., Liu, B. C., Li, J. R. & Yuan, H. L. (2007). Numerical Simulation of Unidirectional Solidification Process of Turbine Blade Castings. *Advanced Materials Research*. 26-28, 947-952. DOI:10.4028/www.scientific.net/AMR.26-28.947.
- [16] Pan, D., Xu, Q. Y., Yu, J., Liu, B. C., Li, J. R., Yuan, H. L. & Jin, H.P. (2013). Numerical simulation of directional solidification of single crystal turbine blade casting. *International Journal of Cast Metals Research*. 21(1-4), 308-312. DOI.org/10.1179/136404608X362151.
- [17] Yang, X.L., Dong, H.B., Wang, W. & Lee, P.D. (2004). Microscale simulation of stray grain formation in investment cast turbine blades. *Materials Science and Engineering: A*. 386(1-2), 129-139. DOI.org/10.1016/j.msea.2004.07.007.
- [18] Gao, S.-F, Liu, L, Zhang, J., Xiao, J.-F., Tang, W.-S, Li, Y.-J. & Nan, Q. (2015). Simulation of stray grain formation at the platform during Ni-base single crystal superalloy DD403 casting. *China Foundry*. 12(2) 118-122.
- [19] Pollock, T.M. & Murphy, W.H. (1996). The breakdown of single-crystal solidification in high refractory nickel–base alloys. *Metallurgical and Materials Transactions A*. 27(4), 1081–1094. DOI: 10.1007/BF02649777.
- [20] Miller, J.D. & Pollock, T.M. (2014). Stability of dendrite growth during directional solidification in the presence of a non-axial thermal field. *Acta Materialia*. 78(10), 23-36. DOI:10.1016/j.actamat.2014.05.040.
- [21] Mills, K.C. (2002). *Recommended values of thermophysical properties for selected commercial alloys*. Cambridge: Woodhead Publishing.
- [22] Mochnacki, B., Suchy, J.S. (1993). *Modeling and simulation of casting solidification*. Warszawa: Wydawnictwo Naukowe PWN. (in Polish).
- [23] Staniszewski, B. (1980). *Heat exchange*. Warszawa: WNT. (in Polish).
- [24] Szeliga, D., Kubiak, K., Motyka, M. & Sieniawski, J. (2016). Directional solidification process of nickel based superalloy castings. Thermal analysis. *Vacuum*. 131(9), 327-342. DOI.org/10.1016/j.vacuum.2016.07.009.
- [25] Elliott, A.J., Tin, S., King, W.T., Huang, S.C., Gigliotti, M.F.X. & Pollock, T.M. (2004). Directional solidification of large superalloy castings with radiation and liquid-metal cooling: A comparative assessment. *Metallurgical and Materials Transactions A*. 35(10), 3221-3231. DOI: 10.1007/s11661-004-0066-z
- [26] Miller, J. D. & Pollock, T. M. (2012). Process simulation for the directional solidification of a tri-crystal ring segment via the bridgman and liquid-metal-cooling processes. *Metallurgical and Materials Transactions A*. 43(7), 2414-2425. DOI: 10.1007/s11661-012-1104-x
- [27] Wilson, B.C., Cutler, E.R. & Fuchs, G.E. (2008). Effect of solidification parameters on the microstructures and properties of CMSX-10. *Materials Science and Engineering A*. 479(4), 356-364. DOI:10.1016/j.msea.2007.07.030.
- [28] Sato, A., Harada, H., Yeh, A.C., Kawagishi, K., Kobayashi T., Koizumi, Y., Yokokawa, T. & Zhang, J.X. (2008). A 5th generation SC superalloy with balanced high temperature properties and processability. *Superalloys 2008* (pp. 131–138). The Mineral Metals and Materials Society. 10.7449/2008/Superalloys_2008_131_138.